

**Role of heavy quarks in light hadron fragmentation**Manuel Epele<sup>\*</sup> and Carlos García Canal<sup>†</sup>*Instituto de Física La Plata, UNLP, CONICET Departamento de Física, Facultad de Ciencias Exactas, Universidad de La Plata, Casilla de Correo 69, La Plata, Argentina*R. Sassot<sup>‡</sup>*Departamento de Física and IFIBA, Facultad de Ciencias Exactas y Naturales, Universidad de Buenos Aires, Ciudad Universitaria, Pabellón 1, 1428 Buenos Aires, Argentina*

(Received 2 May 2016; revised manuscript received 27 June 2016; published 24 August 2016)

We investigate the role of heavy quarks in the production of light flavored hadrons and in the determination of the corresponding nonperturbative hadronization probabilities. We define a general mass variable flavor number scheme for fragmentation functions that accounts for heavy quark mass effects, and perform a global QCD analysis to an up-to-date data set including very precise Belle and *BABAR* results. We show that the mass dependent picture provides a much more accurate and consistent description of the data.

DOI: [10.1103/PhysRevD.94.034037](https://doi.org/10.1103/PhysRevD.94.034037)**I. INTRODUCTION**

The effects of heavy quark masses in hard processes and the appropriate definition of parton probability densities for such species of quarks have been very actively studied in recent years [1]. When a heavy quark participates in a hard process, and the characteristic energy of the process under consideration is not far from the heavy quark mass scale, the most natural choice is to treat these particles as massive throughout the calculation, rather than appeal to the more conventional massless parton approximation. However, when the scale of the process exceeds by far the mass scale of the heavy quarks, not only do mass corrections become negligible, but the all-order resummations implicit in massless parton approaches become crucial. This situation clearly represents a challenge for a precise and consistent comparison of processes occurring at very different energy scales, as necessarily happens in a global QCD analysis designed to extract nonperturbative parton distribution functions (PDFs) [2] or fragmentation functions (FFs) [3,4] from the data. To overcome this problem, in most modern global QCD analyses of data, the so-called general mass variable flavor number (GMVFN) schemes [5–8] for parton densities are introduced, as they allow one to retain the advantages of massive schemes near the mass thresholds and those of the massless approach at high energies, smoothly interpolating between both regimes.

In fact, different GMVFN approaches have been applied to the analysis of fragmentation probabilities of heavy quarks into heavy flavored hadrons [9–12], but until now little attention has been paid in this respect to light hadron

fragmentation processes. Since the charm and bottom content in the proton is rather limited, the production of light mesons via heavy quarks of course is strongly suppressed relative to that via light quarks both in proton-proton collisions and in semi-inclusive deep inelastic scattering (SIDIS). Heavy quark corrections are thus expected to be negligible for these processes. But that is not the case for single inclusive electron-positron annihilation (SIA) into light mesons, where the charm and bottom contribution to the cross section is estimated to be comparable in size to that of the light flavors [13]. Whereas charm and bottom mass corrections may still be negligible in SIA experiments tuned at the mass of the Z boson, they are certainly relevant at the energy scales of the more recent *BABAR* and Belle experiments [14,15], which are just above the bottom mass threshold.

In this paper we compute the single inclusive electron-positron annihilation cross section with nonzero masses for the charm and bottom quarks at first order in the strong coupling constant  $\alpha_s$ , and we estimate the effects of retaining these mass corrections in pion production. Since we find the mass dependence to be large but we want to keep the advantages of the next-to-leading order (NLO) massless approximation at high energies, we define a general mass variable flavor number scheme for fragmentation functions in the lines of the fixed-order-next-to-leading-logarithm (FONLL) scheme [16,17], commonly used for parton distribution functions (PDFs). We implement numerically this scheme in Mellin moment space for the fast computation of the cross sections as required by QCD global analyses, and we perform them including recent Belle and *BABAR* data. The mass dependent picture introduced by the GMVFN scheme is found to be relevant in the extraction of fragmentation functions both in terms of the quality of the fit to data and in the reduction of the

<sup>\*</sup>manuepele@fisica.unlp.edu.ar<sup>†</sup>garcia@fisica.unlp.edu.ar<sup>‡</sup>sassot@df.uba.ar

normalization shifts applied to data that are customarily included in global fits. The shape of the charm into a pion fragmentation function, which contributes significantly to the cross section at the energies of the Belle and *BABAR* experiments, is noticeably modified relative to the results obtained within a massless scheme. The bottom fragmentation, constrained mainly by higher energy data, remains similar to the one found in the massless approximation.

## II. FACTORIZATION SCHEMES

Most analyses of quark fragmentation into light flavored hadrons [3,4] rely on the massless perturbative QCD approximation, supplemented with heavy quark mass thresholds, where the corresponding heavy quarks become active, contribute to cross sections, and enter the scale or evolution equations [18]. This zero mass variable flavor number (ZMVFN) scheme is the simplest framework to compute the SIA cross section [19]:

$$\frac{d\sigma^{\text{ZMVFN}}}{dz} = \sum_{i=q,g,h} \hat{\sigma}_i^{\text{ZM}}(z, Q) \otimes D_i^{\text{ZM}}(z, Q), \quad (1)$$

where  $\hat{\sigma}_i^{\text{ZM}}$  is the massless partonic SIA cross section into a parton of flavor  $i$ , and  $D_i^{\text{ZM}}$  are the corresponding FFs, for which we omit in what follows the dependence on the scaled hadron energy fraction  $z$ .  $\otimes$  represents the appropriate convolution over  $z$ , and  $Q$  is the center of mass energy.  $D_i^{\text{ZM}}$  evolves in the scale  $Q$  through massless QCD evolution equations for any parton flavor  $i$ , which include light ( $q$ ) and heavy ( $h$ ) quarks and antiquarks and gluons ( $g$ ). Equation (1) gives a remarkably good approximation at NLO and next-to-next-to-leading order well above mass threshold  $m_h$  [13,20], i.e.  $Q \gg m_h$ , but fails to account for mass effects. Alternatively, in a massive scheme (M), heavy quark masses are kept at the partonic cross section level,

$$\frac{d\sigma^{\text{M}}}{dz} = \sum_{i=q,g} \hat{\sigma}_i^{\text{M}}(Q, m_h) \otimes D_i^{\text{M}}(Q) + \hat{\sigma}_h^{\text{M}}(Q, m_h) \otimes D_h^{\text{M}}. \quad (2)$$

Light flavored FFs  $D_{q,g}^{\text{M}}(Q)$  still evolve through massless QCD evolution equations in NLO, although heavy quark loops contribute above  $\mathcal{O}(\alpha_s^2)$ , and heavy quark FFs  $D_h^{\text{M}}$  decouple from the QCD evolution [21]. The massive scheme gives a good description near the mass thresholds, but fails to converge to the massless limit at high energies because of potentially large logarithmic contributions [ $\alpha_s^k \log^k(m_h/Q)$ ] present in the partonic cross sections  $\hat{\sigma}_i^{\text{M}}$  that spoil the convergence of the perturbation expansion. These logarithmic contributions are effectively resummed in the renormalization group improved ZM approximation. In fact, it has been shown [22,23] that in the massless limit, i.e.  $Q \gg m_h$ ,

$$\hat{\sigma}_i^{\text{M}}(Q, m_h) \xrightarrow{m_h \rightarrow 0} \sum_{j=q,g,h} \hat{\sigma}_j^{\text{ZM}}(Q) \otimes \mathcal{A}_{ji}(Q/m_h), \quad (3)$$

where all logarithmic contributions can be factorized in an operator matrix  $\mathcal{A}_{ij}$  that is independent of the hard process under consideration [11,12,24].

The advantages of both the zero mass and the massive schemes can be exploited in a general mass (GM) scheme, which defines the corresponding fragmentation probabilities through

$$\frac{d\sigma^{\text{GMVFN}}}{dz} = \sum_{i=q,g,h} \hat{\sigma}_i^{\text{GM}}(Q, m_h) \otimes D_i^{\text{GM}}(Q), \quad (4)$$

where a subtracted massive partonic cross section

$$\hat{\sigma}_j^{\text{GM}}(Q, m_h) = \sum_{i=q,g,h} \hat{\sigma}_i^{\text{M}}(Q, m_h) \otimes \mathcal{A}_{ij}^{-1}(Q/m_h) \quad (5)$$

guarantees the correct massless behavior at high energies. The fragmentation functions  $D_j^{\text{GM}}(Q)$  obey standard evolution equations as in the ZM scheme and the continuity across the thresholds can be ensured by imposing the following matching condition:

$$D_j^{\text{GM}}(m_h) = \sum_{i=q,g,h} \mathcal{A}_{ji}(1) \otimes D_i^{\text{M}}(m_h), \quad (6)$$

analogously as in the FONLL scheme for PDFs [16,17].

In order to illustrate the effects arising from the use of the different approximations for the partonic cross sections, in Fig. 1 we show the charm and bottom contribution to the SIA pion cross section (upper and lower panels, respectively) as a function of the center of mass energy  $Q$  at two reference values of  $z$ . For comparison, the same set of NLO FFs that will be described in detail in the next section is convoluted with the NLO massless (ZM) partonic cross section (red solid lines), the full  $\mathcal{O}(\alpha_s)$  massive (M) result (black dashed lines), and the subtracted (GM) approximation (blue dot-dashed lines). Even though the scheme defined by Eqs. (4)–(6) interpolates between the massive behavior near thresholds and the desired zero mass limit at  $Q \gg m_h$ , this solution is clearly not unique. The same limits can be satisfied in alternative factorization schemes where the convergence to the massless limit happens at a lower or higher energy scale. For instance, substituting

$$\hat{\sigma}_j^{\text{GM}} \rightarrow \hat{\sigma}_j^{\text{GM}^*} = (1 - f(Q))\hat{\sigma}_j^{\text{M}} + f(Q)\hat{\sigma}_j^{\text{GM}} \quad (7)$$

into Eq. (4), with an  $f(Q)$  that vanishes in the threshold  $f(m_h) = 0$ , and saturates to 1 for  $Q \gg m_h$  such that  $f(Q) = 1 - 2m_h/Q$ , would delay the onset of the masslesslike behavior, as shown for the charm contribution by the grey dotted lines in the upper panels of Fig. 1, while

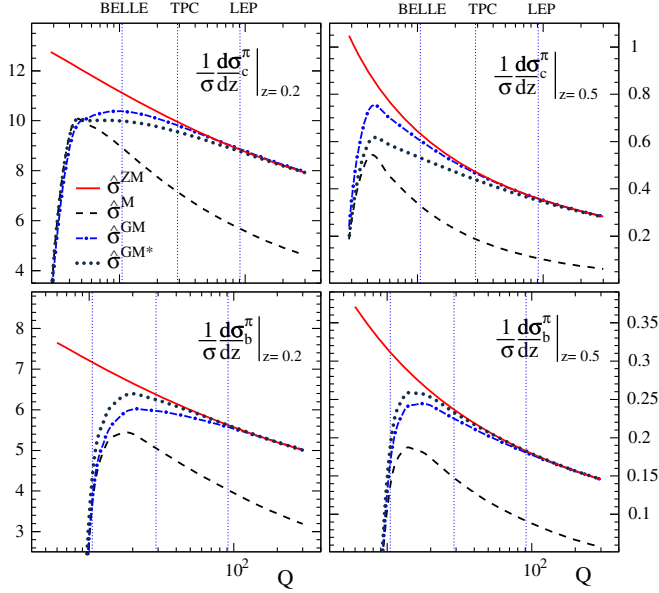


FIG. 1. Charm and bottom contribution to the SIA cross section computed with different approximations for the partonic cross sections and the same set of FFs.

$$\hat{\sigma}_j^{\text{GM}} \rightarrow \hat{\sigma}_j^{\text{GM}^*} = (1 - f(Q))\hat{\sigma}_j^{\text{GM}} + f(Q)\hat{\sigma}_j^{\text{ZM}} \quad (8)$$

would suppress mass effects, as shown for the bottom contribution in the lower panels. In any case, it is clear that while the GM schemes introduce negligible corrections at the energy scale of the LEP experiments, mass effects are significant at the scales of Belle and *BABAR*. The remarkably precise measurements of the SIA cross section as a function of  $z$  performed by these experiments allows one to check whether a particular scheme is favored by the data.

### III. GMVFN SCHEME GLOBAL ANALYSIS FOR FFs

In this section, we discuss the actual relevance of heavy quark mass corrections in charged pion production, implementing different factorization schemes in a NLO QCD global analysis for the extraction of FFs, performed along the lines of that of Ref. [13]. The method for the global analysis has been described in detail in [3,13]. It is based on an efficient Mellin moment technique that allows one to tabulate and store the computationally most demanding parts of the NLO calculation of SIA, SIDIS, and proton-proton hadroproduction cross sections prior to the actual analysis. In this way, the evaluation of the relevant cross sections becomes so fast that it can be easily performed inside a standard  $\chi^2$  minimization. At variance with [13], where SIA cross sections were evaluated only in the ZM approximation, here they are extended to the GM framework, which requires one to define different contours in the complex moment space to perform the Mellin inversion. Hadroproduction and SIDIS cross sections are still

computed in the ZM framework, to assess in this first step the impact introduced by SIA corrections. Nevertheless, the heavy quark contributions to these processes are negligibly small. Also a minor difference with [13] is that we remove from the data sets included in the analysis TASSO and OPAL light flavor tagged data, which have comparatively large errors.

In Table I we compare the quality of a fit performed within the standard ZMVFN factorization scheme, and a GMVFN variant where the prescriptions of Eqs. (7) and (8) have been adopted for the charm and bottom coefficients, respectively, as in the example of Fig. 1. Among the different prescriptions we have explored, the above mentioned one reproduces best the data, significantly better than in the ZMVFN scheme, with much lower  $\chi_i^2$  per data values and smaller normalization shifts  $N_i$ . No significant improvement is found with more sophisticated weight functions  $f(Q)$ . On the other hand, the most simple subtraction of Eq. (5) produces fits of much poorer quality, suggesting that such prescription oversubtracts for charm, and converges much slower to the massless limit than the data require for bottom.

As expected, heavy quark mass effects are most noticeable for Belle and *BABAR* experiments, since at their relatively low center of mass energies heavy quarks are far from behaving as massless. On the other hand, even though these experiments are above the bottom threshold

TABLE I. Individual  $\chi^2$  values and normalization shifts  $N_i$  for the data sets included in global analyses where the ZMVFN and GMVFN schemes have been implemented.

Experiment	Data type	No. data in fit	ZMVFN $N_i$	ZMVFN $\chi^2/\text{data}$	GMVFN $N_i$	GMVFN $\chi^2/\text{data}$
ALEPH [25]	inclusive	22	0.968	0.982	0.994	1.059
<i>BABAR</i> [14]	inclusive	39	1.019	1.967	1.002	1.492
Belle [15]	inclusive	78	1.044	0.250	1.019	0.141
DELPHI [26]	inclusive	17	0.978	0.394	1.003	0.547
	<i>uds</i> tag	17	0.978	1.224	1.003	0.559
	<i>b</i> tag	17	0.978	0.618	1.003	0.459
OPAL [27]	inclusive	21	0.946	1.329	0.970	0.757
SLD [28]	inclusive	28	0.938	1.000	0.963	0.696
	<i>uds</i> tag	17	0.938	1.253	0.963	0.665
	<i>c</i> tag	17	0.938	2.000	0.963	1.165
	<i>b</i> tag	17	0.938	0.653	0.963	0.582
TPC [29]	inclusive	17	0.997	1.865	1.006	1.641
	<i>uds</i> tag	9	0.997	0.222	1.006	0.222
	<i>c</i> tag	9	0.997	0.656	1.006	0.478
	<i>b</i> tag	9	0.997	1.067	1.006	1.211
COMPASS [30]	$\pi^\pm$ (d)	398	1.003	0.952	1.008	0.962
HERMES [31]	$\pi^\pm$ (p)	64	0.981	1.156	0.986	1.092
	$\pi^\pm$ (d)	64	0.980	1.677	0.985	1.620
PHENIX [32]	$\pi^0$	15	1.174	0.953	1.167	0.960
STAR [33]	$\pi^\pm, \pi^0$	38	1.205	0.821	1.202	0.889
ALICE [34]	$\pi^0$	11	0.696	3.027	0.700	2.836
TOTAL:		924		$\chi^2/\text{dof} = 1.079$		$\chi^2/\text{dof} = 0.977$

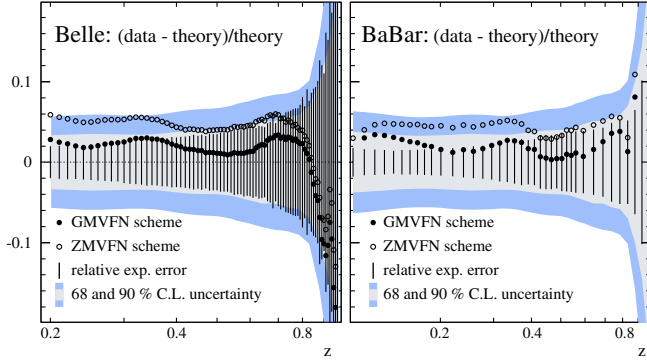


FIG. 2. Comparison between data from Belle and *BABAR* and estimates from the ZMVFN and GMVFN schemes.

$2m_b$ , where the bottom should be considered as an active flavor in the ZMVFN scheme, the bottom is actually strongly suppressed, a feature that is well accounted for in the GMVFN scheme. In Fig. 2 we show the differences between the fit estimates and Belle and *BABAR* data, against the relative experimental error. The 68% and 90% C.L. limit bands for the GMVFN estimates are also included.

Notice that there is also a considerable improvement in the description of data from experiments at a higher energy scale. The difference between the massless and the mass dependent picture comes in this case from the fact that the QCD scale dependence preserves the difference between the charm fragmentation probabilities constrained by lower energy data, as shown in Fig. 3. The bottom fragmentation probability is mainly constrained by high energy flavor tagged SIA data, for which mass dependent corrections become negligible, and therefore the results for this flavor in both pictures agree. The GMVFN however guarantees that the bottom contribution at lower energies is conveniently suppressed, improving the overall agreement and consistency. No significant differences are found for the light flavors, which are constrained mainly by light flavor tagged SIA and SIDIS data.

It is worthwhile mentioning that heavy quark fragmentation functions into pions are found to be larger than those corresponding to the light flavors both in the GMVFN and the ZMVFN approximations, and as in previous ZMVFN analyses. This suggests not only that the perturbative coefficients we have computed are strongly dependent on the quark masses, but also that the nonperturbative hadronization mechanisms encoded in the fragmentation functions are clearly sensitive to the quark masses. In this

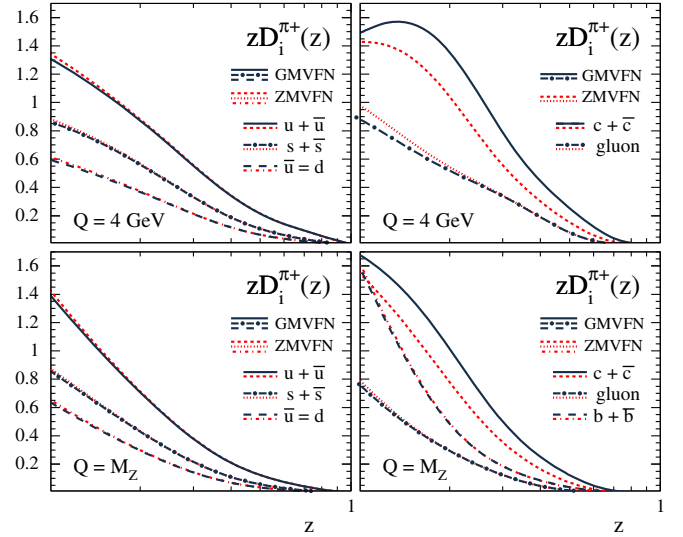


FIG. 3. FFs at  $Q = 4 \text{ GeV}$  and  $Q = M_Z$  coming from the ZMVFN and GMVFN schemes.

picture, massive quarks would have more strong decay channels than their almost massless counterparts.

#### IV. CONCLUSIONS AND OUTLOOK

We have shown that an accurate determination of the fragmentation probabilities of quarks and gluons into pions, matching the precision of the present generation of hadroproduction experiments, requires a picture sensitive to heavy quark dynamics. Such a picture was presented here, together with the results of a NLO QCD global analysis where it was implemented. Heavy quark mass dependence is especially relevant in single inclusive electron-positron annihilation into pions, where the detailed energy scale dependence of the charm contribution and the suppression of the bottom above their respective thresholds is non-negligible. These effects are expected to be even more apparent in global fits to data on the production of heavy flavored mesons from different observables at different energy scales, where the mass dependent fragmentation probabilities are dominant.

#### ACKNOWLEDGMENTS

We warmly acknowledge Daniel de Florian and Marco Stratmann for their help and encouragement. This work was supported by CONICET, ANPCyT and UBACyT.

- [1] See, e.g. R. D. Ball, M. Bonvini, and L. Rottoli, Charm in deep-inelastic scattering, *J. High Energy Phys.* **11** (2015) 122, and references therein.
- [2] For a review see, e.g. J. Rojo *et al.*, The PDF4LHC report on PDFs and LHC data: Results from Run I and preparation for Run II, *J. Phys. G* **42**, 103103 (2015).
- [3] D. de Florian, R. Sassot, and M. Stratmann, Global analysis of fragmentation functions for pions and kaons and their uncertainties, *Phys. Rev. D* **75**, 114010 (2007).
- [4] S. Albino, B. A. Kniehl, and G. Kramer, Fragmentation functions for light charged hadrons with complete quark flavor separation, *Nucl. Phys. B* **725**, 181 (2005); AKK update: Improvements from new theoretical input and experimental data, *Nucl. Phys. B* **803**, 42 (2008); M. Hirai, S. Kumano, T.-H. Nagai, and K. Sudoh, Determination of fragmentation functions and their uncertainties, *Phys. Rev. D* **75**, 094009 (2007).
- [5] M. A. G. Aivazis, J. C. Collins, F. I. Olness, and W. K. Tung, Leptoproduction of heavy quarks. II. A unified QCD formulation of charged and neutral current processes from fixed target to collider energies, *Phys. Rev. D* **50**, 3102 (1994).
- [6] R. S. Thorne and R. G. Roberts, A variable number flavor scheme for charged current heavy flavor structure functions, *Eur. Phys. J. C* **19**, 339 (2001).
- [7] R. S. Thorne, A variable-flavor number scheme for NNLO, *Phys. Rev. D* **73**, 054019 (2006).
- [8] M. Guzzi, P. M. Nadolsky, H. L. Lai, and C.-P. Yuan, General-mass treatment for deep inelastic scattering at two-loop accuracy, *Phys. Rev. D* **86**, 053005 (2012).
- [9] M. Cacciari, P. Nason, and C. Oleari, Crossing heavy-flavor thresholds in fragmentation functions, *J. High Energy Phys.* **10** (2005) 034.
- [10] M. Cacciari, P. Nason, and C. Oleari, A study of heavy flavoured meson fragmentation functions in  $e^+e^-$  annihilation, *J. High Energy Phys.* **04** (2006) 006.
- [11] T. Kneesch, B. A. Kniehl, G. Kramer, and I. Schienbein, Charmed-meson fragmentation functions with finite-mass corrections, *Nucl. Phys. B* **799**, 34 (2008).
- [12] B. A. Kniehl, G. Kramer, I. Schienbein, and H. Spiesberger, Finite-mass effects on inclusive  $B$  meson hadroproduction, *Phys. Rev. D* **77**, 014011 (2008).
- [13] D. de Florian, R. Sassot, M. Epele, R. J. Hernández-Pinto, and M. Stratmann, Parton-to-pion fragmentation reloaded, *Phys. Rev. D* **91**, 014035 (2015).
- [14] J. P. Lees *et al.* (BABAR Collaboration), Production of charged pions, kaons and protons in  $e^+e^-$  annihilations into hadrons at  $\sqrt{s} = 10.54$  GeV, *Phys. Rev. D* **88**, 032011 (2013).
- [15] M. Leitgab *et al.* (Belle Collaboration), Precision Measurement of Charged Pion and Kaon Multiplicities in Electron-Positron Annihilation at  $Q = 10.52$  GeV, *Phys. Rev. Lett.* **111**, 062002 (2013).
- [16] S. Forte, E. Laenen, P. Nason, and J. Rojo, Heavy quarks in deep-inelastic scattering, *Nucl. Phys. B* **834**, 116 (2010).
- [17] R. D. Ball, V. Bertone, M. Bonvini, S. Forte, P. G. Merrill, J. Rojo, and L. Rottoli, Intrinsic charm in a matched general-mass scheme, *Phys. Lett. B* **754**, 49 (2016).
- [18] G. Altarelli and G. Parisi, Asymptotic freedom in parton language, *Nucl. Phys. B* **126**, 298 (1977); Y. L. Dokshitzer, Calculation of the structure functions for deep inelastic scattering and  $e^+e^-$  annihilation by perturbation theory in quantum chromodynamics, *Zh. Eksp. Teor. Fiz.* **73**, 1216 (1977) [*Sov. Phys. JETP* **46**, 641 (1977)]; V. N. Gribov and L. N. Lipatov, Deep inelastic  $ep$  scattering in perturbation theory, *Sov. J. Nucl. Phys.* **15**, 438 (1972).
- [19] G. Altarelli, R. K. Ellis, G. Martinelli, and S. Y. Pi, Processes involving fragmentation functions beyond the leading order in QCD, *Nucl. Phys. B* **160**, 301 (1979).
- [20] D. P. Anderle, F. Ringer, and M. Stratmann, Fragmentation functions at next-to-next-to-leading order accuracy, *Phys. Rev. D* **92**, 114017 (2015).
- [21] J. C. Collins, Hard scattering factorization with heavy quarks: A general treatment, *Phys. Rev. D* **58**, 094002 (1998).
- [22] M. Buza, Y. Matiounine, J. Smith, and W. L. van Neerven, Charm electroproduction viewed in the variable flavor number scheme versus fixed order perturbation theory, *Eur. Phys. J. C* **1**, 301 (1998).
- [23] I. Bierbaum, J. Blumlein, and S. Klein, The gluonic operator matrix elements at  $O(\alpha_s^2)$  for DIS heavy flavor production, *Phys. Lett. B* **672**, 401 (2009).
- [24] B. A. Kniehl, G. Kramer, I. Schienbein, and H. Spiesberger, Inclusive  $D^{*\pm}$  production in  $p\bar{p}$  collisions with massive charm quarks, *Phys. Rev. D* **71**, 014018 (2005); Collinear subtractions in hadroproduction of heavy quarks, *Eur. Phys. J. C* **41**, 199 (2005).
- [25] D. Buskulic *et al.* (ALEPH Collaboration), Inclusive  $\pi^\pm$ ,  $K^\pm$  and  $(p\bar{p})$  differential cross-sections at the  $Z$  resonance, *Z. Phys. C* **66**, 355 (1995).
- [26] P. Abreu *et al.* (DELPHI Collaboration),  $\pi^\pm$ ,  $K^\pm$ ,  $p$  and  $\bar{p}$  production in  $Z0 \rightarrow q\bar{q}$ ,  $Z0 \rightarrow b\bar{b}$ ,  $Z0 \rightarrow u\bar{u}$ ,  $d\bar{d}$ ,  $s\bar{s}$ , *Eur. Phys. J. C* **5**, 585 (1998).
- [27] R. Akers *et al.* (OPAL Collaboration), Measurement of the production rates of charged hadrons in  $e^+e^-$  annihilation at the  $Z0$ , *Z. Phys. C* **63**, 181 (1994).
- [28] K. Abe *et al.* (SLD Collaboration), Production of  $\pi^\pm$ ,  $K^\pm$ ,  $K0$ ,  $K^{*0}$ ,  $\phi$ ,  $p$  and  $\Lambda^0$  in hadronic  $Z^0$  decays, *Phys. Rev. D* **59**, 052001 (1999).
- [29] H. Aihara *et al.* (TPC/Two Gamma Collaboration), Pion and kaon multiplicities in heavy quark jets from  $e^+e^-$  annihilation at 29 GeV, *Phys. Lett. B* **184**, 299 (1987); Charged Hadron Inclusive Cross Sections and Fractions in  $e^+e^-$  Annihilation  $\sqrt{s} = 29$  GeV, *Phys. Rev. Lett.* **61**, 1263 (1988).
- [30] N. Makke (for the COMPASS Collaboration), Fragmentation functions measurement at COMPASS, *Proc. Sci., DIS2013* (2013) 202.
- [31] A. Airapetian *et al.* (HERMES Collaboration), Multiplicities of charged pions and kaons from semi-inclusive deep-inelastic scattering by the proton and the deuteron, *Phys. Rev. D* **87**, 074029 (2013).
- [32] A. Adare *et al.* (PHENIX Collaboration), Inclusive cross-section and double helicity asymmetry for  $\pi^0$  production in  $p + p$  collisions at  $\sqrt{s} = 200$  GeV: Implications for the polarized gluon distribution in the proton, *Phys. Rev. D* **76**, 051106 (2007).
- [33] L. Adamczyk *et al.* (STAR Collaboration), Neutral pion cross section and spin asymmetries at intermediate pseudorapidity in polarized proton collisions at  $\sqrt{s} = 200$  GeV, *Phys. Rev. D* **89**, 012001 (2014).
- [34] B. Abelev *et al.* (ALICE Collaboration), Neutral pion and  $\eta$  meson production in proton-proton collisions at  $\sqrt{s} = 0.9$  TeV and  $\sqrt{s} = 7$  TeV, *Phys. Lett. B* **717**, 162 (2012).